

Measurements of Total Neutron Cross Sections of C, Fe, Pb, O, Mo, Si, Zn, Ni, Sn, Ti and W at Energies 20–60 MeV

By

Kazuo Shin*, Yoshiaki Ishii*, Yoshitomo Uwamino**,
Hideyuki Sakai*** and Shigeo Numata****

(Received March 25, 1993)

Abstract

Measurements of total neutron cross sections of C, Fe, Pb, O, Mo, Si, Zn, Ni, Sn, Ti and W were made, using white neutrons from a thick Cu target bombarded by 65- and 75-MeV protons. The cross sections were obtained in the energy range 20–60 MeV.

The obtained data agree well with others in the case where other data were already existing. The present work added several new data points for Ni, Mo, Sn, Zn, Ti and W, for which the number of existing data was not enough.

I. Introduction

Recently, neutron cross sections at energies beyond 15 MeV are gathering more interest as the application of high energy accelerators is being planned in the area of the actinide transmutation and fusion material damage study. The radiation shielding of these high energy accelerators needs accurate cross sections above 15 MeV to about 100 MeV. Beyond this energy the systematic calculation based on an intra-nuclear cascade code gave satisfactory results for shielding purposes.

Previously we made neutron transmission experiments through several materials by neutrons of energies up to 30 MeV./1–3/ Recently the experiment was expanded to higher energy up to 75 MeV./4/ Several discrepancies were found in neutron spectra transmitted through iron and lead shields between the new experiment and the calculation based on the DLC-87 multigroup cross sections./5/ The neutron fluxes in the above experiment were very sensitive to

* Department of Nuclear Engineering, Kyoto University, Yoshida-honmachi, Sakyo-ku, Kyoto 606, Japan

** Institute for Nuclear Study, University of Tokyo, Midori-cho, Tanashi, Tokyo 188, Japan

*** Department of Physics, University of Tokyo, Hongoh, Bunkyo-ku, Tokyo 113, Japan

**** Shimizu Corporation, Etchu-jima, Koto-ku, Tokyo 135, Japan

total and nonelastic cross sections of the shield materials. The accuracy of these data seemed suspicious to us, and it seemed necessary to perform a new measurement of these data. As the first step of this, the measurement of the total cross sections was planned, since the measurement of the total cross sections was easier than the experiment for the nonelastic cross sections.

In the measurement, materials which were more important for engineering use, or materials for which the past cross section measurements seemed to be not sufficient, were taken up. Examples of the first type of materials are C, O, Fe, Pb, Si, and materials selected for the second reason are Mo, Zn, Ni, Sn, Ti and W. The neutron energy range covered by this experiment is from 20 MeV to about 60 MeV.

II. Experimental Method

The measurement was performed at the AVF cyclotron facility of Osaka University. Protons accelerated by the cyclotron to 65 MeV or 75 MeV were injected onto a 1-cm thick (beam stopping range) Cu target. Neutrons generated from the Cu target in the forward direction were pulled out to an experimental room through a 7.5-cm diameter by 50-cm long concrete collimator. Figure 1 shows the experimental setup.

The neutron spectra emitted at 0° from the Cu target are plotted in Fig. 2. The neutrons were detected by a 7.6-cm diameter by 7.6-cm long NE-213 scintillator at a location 778 cm down from the Cu target. Thin samples of different thicknesses were inserted in the neutron beam at a 30-cm distance from the collimator exit, and the attenuation of neutrons at various energies was detected by the time-of-flight (TOF) method.

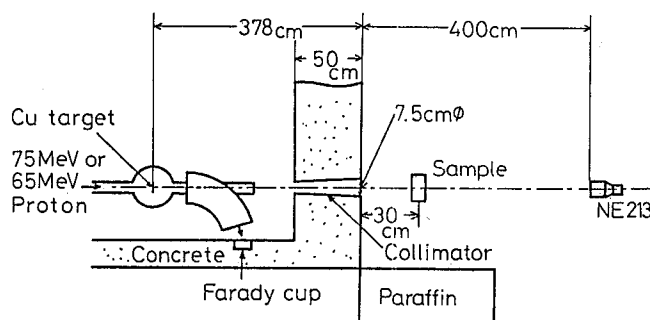


Fig. 1 Experimental setup for the cross section measurements.

In the measurement, signals for the flight time, the rise time and pulse height were stored in the list mode. The data were offline analyzed after the experiment. The resolution of the energy measurement by the TOF method was about 3 MeV at 65-MeV neutron energy for the 778-cm flight path arrangement.

The sample materials and their sizes are listed in Table I as well as the proton energy and the flight path length. The experiment was performed in three separated series of runs, the proton acceleration energy being 65 MeV or 75 MeV and the flight path length being 543 cm or 778 cm.

A water sample was used for the measurement of oxygen cross sections. The water was filled in a thin (0.5-mm thickness) Al can. For the correction of the attenuation by the Al can, the measurement was repeated with the empty Al can.

The amount of the background, mostly neutrons penetrating through the collimator wall, was measured with an iron plug in the collimator. It was found that the intensity of the background neutrons was more than three orders of magnitude less than the beam neutrons. So they were neglected in the analysis.

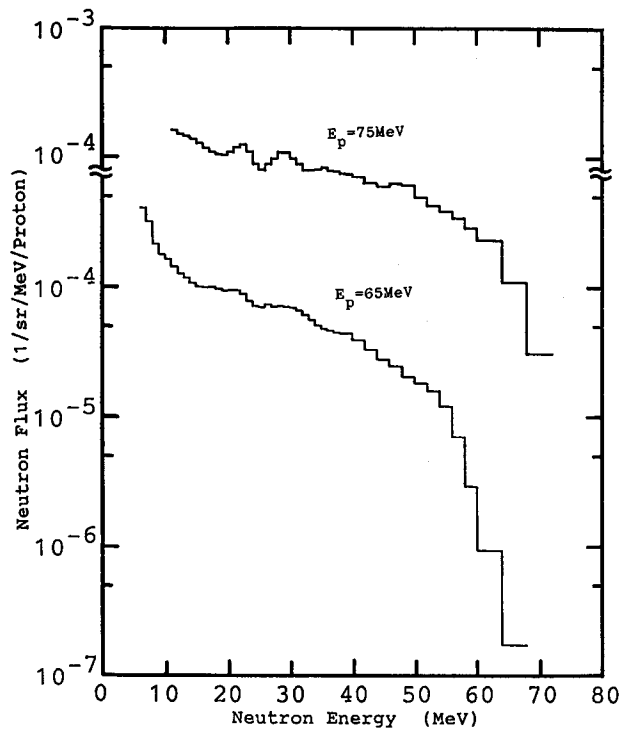


Fig. 2 Source neutron spectra used for the cross section measurements.

Table I List of Sample Dimension and Experimental Conditions Used in the Cross Section Measurements

Material	Thickness (cm)	Size (cm)	Flight Path (cm)	Proton Energy (MeV)
C	1,3,5	20 diam.	543	65
Fe	1,3,5	22 × 22	778	75
Pb	1,3,5	15 × 15	778	75
Si	1,3,5	10 diam.	778	75
Mo	2,4,6	10 diam.	778	75
H ₂ O	4,10,18	20 × 20	778	75
Zn	1,3,5	10 diam.	778	65
Ni	1,3,5	10 diam.	778	65
Sn	1,3,5	10 diam.	778	65
Ti	1,3,5	10 diam.	778	65
W	0.3,0.6,0.9	15 diam.	778	65

III. Data Analysis Method

The proton beam repetition rate at the Cu target was not variable. It was 1/55 ns. Under this restriction, low energy neutrons below 20 MeV were caught up by high energy neutrons of the next flash, and their signals contaminated the TOF spectrum of lower energy neutrons. To remove these low energy neutrons from the time spectrum, pulse-height signals were utilized. Neutron time signals which had a pulse height higher than 20 MeV in recoiled proton energy were picked up. The obtained time spectrum which corresponded to neutron energy above 20 MeV was obviously distorted by the detector efficiency biased by the discrimination at the 20 MeV proton energy. However the information needed to obtain the total cross section was the relative attenuation rate of the neutron count at each flight time.

The time spectrum was bunched into energy bins with the 5-MeV width, and the total cross section (averaged over the energy bin) was obtained from the decreasing rate of the neutron count at each energy bin.

The count $C_0(E)$ of source neutrons at the energy E per incident proton, and the count $C(E, t_j)$ obtained when the sample of the thickness t_j is set, are related to each other with the total cross section $\sigma_t(E)$,

$$C(E, t_j)dE = C_0(E) \exp \{ -N\sigma_t(E)t_j \} dE, \quad (1)$$

where N is the atomic density in the sample. The equation (2),

$$\ln C(E, t_j) = \ln C_0(E) - N\sigma_t(E)t_j \quad (2)$$

was fitted to the measured data by the least square method with the weight,

$$W(E, t_j) = 1/\{S(E, t_j)\}^2, \quad (3)$$

where

$$S(E, t_j) = \delta C(E, t_j)/C(E, t_j), \quad (4)$$

and $\delta C(E, t_j)$ is the statistical error in the $C(E, t_j)$.

From the error propagation, the estimated error in the obtained $\sigma_t(E)$ value is

$$\delta\sigma_t(E) = \frac{1}{N} \sqrt{\frac{1}{D(E)} \sum_j \frac{1}{\{S(E, t_j)\}^2}}, \quad (5)$$

and

$$D(E) = \left\{ \sum_j W(E, t_j) \right\} \left\{ \sum_j W(E, t_j) t_j^2 \right\} - \left\{ \sum_j W(E, t_j) t_j \right\}^2. \quad (6)$$

The 5-MeV energy width was decided from the consideration of both the statistical error $\delta C(E, t_j)$ and the energy resolution in the TOF measurement.

Oxygen cross sections were derived by subtraction of the hydrogen cross sections in Ref. 6 from the obtained total cross sections of water. No error was assigned to the hydrogen cross sections.

IV. Results

The deduced total cross section data as well as their error values are listed in Table II. Some of data are also plotted in Figs. 3 through 9 in comparison with other data from BNL-325./7/

Figure 3 shows the σ_t data for carbon. Our data agree very well with those of Peterson/8/, Auman/7/ and the DLC-87 file/5/ showing the accuracy of our measurement.

The number of data points in the W cross section data becomes smaller in BNL-325 as shown in Fig. 4, as the neutron energy exceeds 15 MeV, in particular above 30 MeV. The data obtained in this work are on a smoothly

Table II List of Obtained Total Cross Sections

Material	Cross Sections (barns)									
	E_n^* (MeV)	22.5	27.5	32.5	37.5	42.5	47.5	52.5	57.5	62.5
C	1.409	1.342	1.295	1.115	1.056	1.085	0.950	0.859	0.732	
Error	0.069	0.049	0.046	0.045	0.044	0.045	0.047	0.058	0.023	
Fe	2.598	2.322	2.250	2.346	2.461	2.447	2.393	2.282	2.267	
Error	0.120	0.090	0.060	0.054	0.054	0.056	0.063	0.073	0.086	
Pb	5.806	5.141	4.800	4.698	4.382	4.371	4.416	4.616	—	
Error	0.214	0.140	0.123	0.120	0.123	0.139	0.162	0.193	—	
Mo	3.230	2.945	2.878	2.890	3.100	3.081	3.055	—	—	
Error	0.098	0.073	0.049	0.044	0.046	0.052	0.060	—	—	
O	1.626	1.535	1.400	1.393	1.267	1.200	1.158	1.076	0.975	
Error	0.089	0.063	0.040	0.035	0.033	0.034	0.037	0.042	0.048	
Si	1.997	1.985	1.784	1.937	1.929	1.829	1.797	—	—	
Error	0.209	0.132	0.102	0.101	0.104	0.107	0.117	—	—	
Zn	2.540	2.551	2.502	2.602	2.705	2.815	—	—	—	
Error	0.061	0.046	0.042	0.046	0.052	0.060	—	—	—	
Sn	3.741	3.624	3.337	3.253	3.258	—	—	—	—	
Error	0.097	0.072	0.065	0.071	0.079	—	—	—	—	
Ti	2.279	2.280	2.312	2.330	—	—	—	—	—	
Error	0.060	0.047	0.041	0.045	—	—	—	—	—	
W	5.201	5.085	4.502	4.340	4.227	—	—	—	—	
Error	0.291	0.218	0.199	0.216	0.240	—	—	—	—	

* Midpoint of neutron energy interval (5 MeV).

extrapolated line of other data from the low energy range, and agree well with one existing data at 42 MeV.

A similar thing is pointed out for the total cross section data of Sn shown in Fig. 5, and for those of Ni (not shown in the figure).

Our data of Zn agree fairly well with others in BNL-325, as compared in Fig. 6, although only a few sets of data are existing in BNL-325 in the energy range 20–60 MeV.

Figure 7 showed the data of Ti. There exist no data in the BNL-325 at energies 30 MeV to 60 MeV, where this work provides a few data points. However, data beyond 40 MeV were not obtained in this experiment since the statistics in the measurement were too bad.

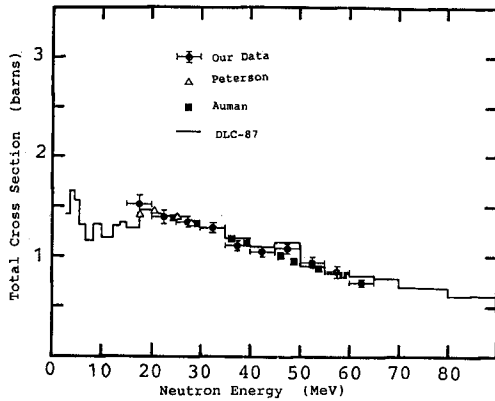


Fig. 3 Total cross sections of C.

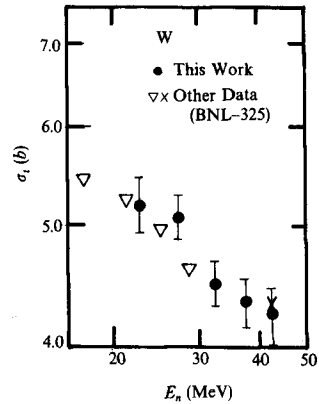


Fig. 4 Total cross sections of W.

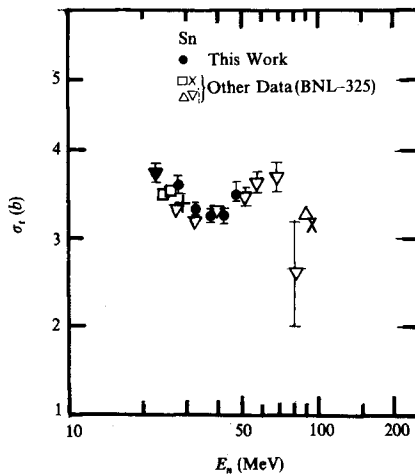


Fig. 5 Total cross sections of Sn.

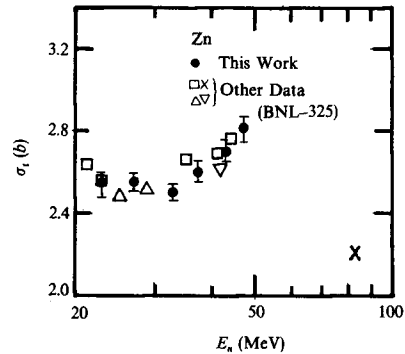


Fig. 6 Total cross sections of Zn.

The total cross sections of Mo are plotted in Fig. 8. The present data, obtained in the energy range of up to 55 MeV, are in good agreement with others in the relative variation in the data with the energy, but slightly smaller than others.

Figure 9 is the plot of the lead cross sections. Our value at 37.5 MeV rises slightly higher than the data of Peterson/8/. Except this, our data are in good agreement with his data. The data of the DLC-87 file are very different from those of the experiments. The file ignored the elastic scattering above 15 MeV

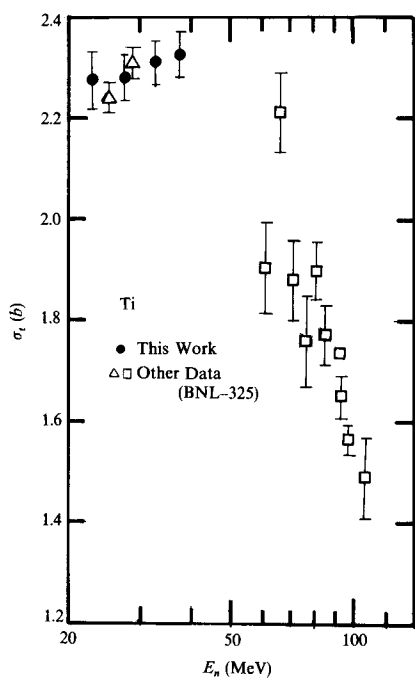


Fig. 7 Total cross sections of Ti.

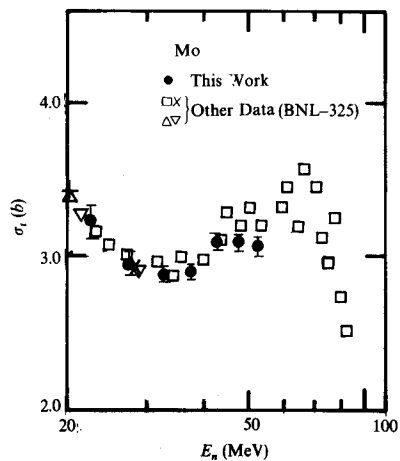


Fig. 8 Total cross sections of Mo.

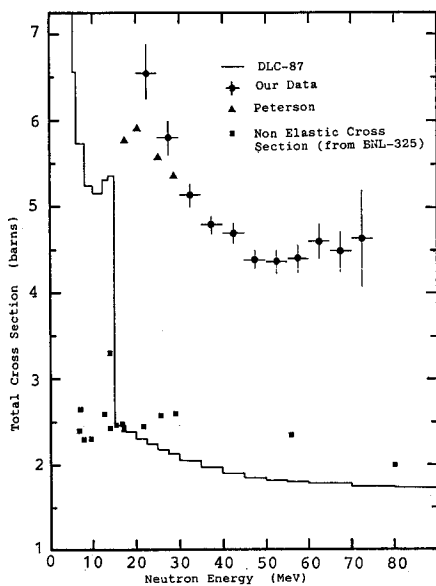


Fig. 9 Total cross sections of Pb.

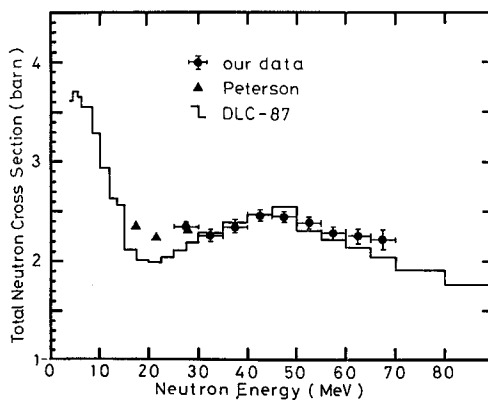


Fig. 10 Total cross sections of Fe.

and used nonelastic cross section values as those of the total cross section for this material (See Fig. 9). Consequently, it largely overpredicted the transmitted neutron spectra through lead shields./4/

Figure 10 shows the data of iron. The present data are in good agreement with Peterson's experimental data/8/. The DLC-87 data are smaller than the experimental data in the energy range of 15–30 MeV. It was found that the iron transmitted neutron spectra were overpredicted by the DLC-87 based calculation at energies corresponding to the above energy range./4/.

V. Conclusions

The present data agreed well with others in the cases where other data existed. The present work added several new data points for Ni, Mo, Sn, Zn, Ti and W, for which the existing data were very few in the BNL-325 file.

References

- 1) K. Shin et al., Bull. Inst. Chem. Res., Kyoto Univ., 57, 102 (1979).
- 2) K. Shin et al., Nucl. Sci. Eng., 71, 294 (1979).
- 3) Y. Uwamino, T. Nakamura and K. Shin, Nucl. Sci. Eng., 80, 360 (1982).
- 4) K. Shin et al., Red. Protec. Dosim., 37, 175 (1991).
- 5) R.G. Alsmiller, Jr. and J. Barish, Nucl. Sci. Eng., 80, 448 (1982).
- 6) A.D. Guerra, Nucl. Instr. & Methods, 135, 337 (1976).
- 7) D.I. Garber and R.R. Kinsey, "BNL-325 Third Edition, Volume II" (1976).
- 8) J.M. Peterson et al., Phys. Rev., 120, 521 (1960).